

# Rotational Fluctuation of the Sodium-driven Flagellar Motor of *Vibrio alginolyticus* Induced by Binding of Inhibitors

Kazumasa Muramoto<sup>1</sup>, Yukio Magariyama<sup>2</sup>, Michio Homma<sup>1</sup>  
Ikuro Kawagishi<sup>1</sup>, Shigeru Sugiyama<sup>2</sup>, Yasuo Imae<sup>1</sup> and  
Seishi Kudo<sup>2,3\*</sup>

<sup>1</sup>Department of Molecular Biology, Faculty of Science Nagoya University Chikusa-Ku Nagoya 464-01 Japan

<sup>2</sup>Tsukuba Research Laboratory, Yaskawa Electric Corporation, 5-9-10 Tokodai Tsukuba 300-26, Japan

<sup>3</sup>PRESTO (Precursory Research for Embryonic Science and Technology) JRDC (Research Development Corporation of Japan) 5-9-10 Tokodai, Tsukuba 300-26, Japan

Rotation of the Na<sup>+</sup>-driven flagellar motor of *Vibrio alginolyticus* was investigated under the influence of inhibitors specific to the motor, amiloride and phenamil. The rotation rate of a single flagellum on a cell stuck to a glass slide was examined using laser dark-field microscopy. In the presence of 50 mM NaCl, the average rotation rate ( $\bar{\omega}$ ) was about 600 r.p.s. with a standard deviation ( $\sigma_{\omega}$ ) of 9% of  $\bar{\omega}$ . When  $\bar{\omega}$  was decreased to about 200 r.p.s. by the presence of 1.5 mM amiloride,  $\sigma_{\omega}$  increased to 15% of  $\bar{\omega}$ . On the other hand, when  $\bar{\omega}$  was decreased to about 200 r.p.s. by the addition of 0.6  $\mu$ M phenamil, a large increase in  $\sigma_{\omega}$  up to 50% of  $\bar{\omega}$ , was observed. Similarly large fluctuations were observed at other concentrations of phenamil. These observations suggest that dissociation of phenamil from the motor was much slower than that of amiloride. A very low concentration of phenamil caused a transient but substantial reduction in rotation rate. This might suggest that binding of only a single molecule of phenamil strongly inhibits the torque generation in the flagellar motor.

© 1996 Academic Press Limited

**Keywords:** flagella; laser dark-field microscopy; amiloride; phenamil; *Vibrio*

\*Corresponding author

## Introduction

Flagellar motors embedded in the cytoplasmic membrane of bacteria convert the electrochemical potential gradient of specific ions into torque (reviewed by Imae & Atsumi, 1989; Blair, 1990). Proton is used as the coupling ion of the motors of neutrophilic bacteria such as *Bacillus subtilis*, *Streptococcus* sp. and *Escherichia coli* (Matsuura *et al.*, 1977; Manson *et al.*, 1977). Sodium ion is used in alkaliphilic *Bacillus* spp. and some *Vibrio* spp. (Hirota *et al.*, 1981; Chernyak *et al.*, 1983; Atsumi *et al.*, 1992b).

The components of the motor, “force-generating

units” have the ability to translocate the coupling ion and generate torque through their interaction with some rotor elements (reviewed by Jones & Aizawa, 1991; Khan, 1993). Previous studies have shown that a single motor has multiple independently functioning force-generating units (Block & Berg, 1984; Blair & Berg, 1988; Muramoto *et al.*, 1994). In the H<sup>+</sup>-driven motor of *E. coli*, the presence of eight units in a fully functioning motor was suggested by experiments involving successive incorporation of subunits of the motor proteins, MotA and MotB (Blair & Berg, 1988). In the Na<sup>+</sup>-driven motor of *Bacillus firmus*, the presence of five to nine units was suggested by irreversible inactivation by a photoreactive amiloride analog, 6-iodoamiloride (6-IA; Muramoto *et al.*, 1994). Electron microscopic studies also suggested that there are several ring particles, which might correspond to the force-generating units, in the cytoplasmic membranes of *E. coli*, *Salmonella typhimurium*, *B. firmus*, *B. subtilis*, *Aquaspirillum serpens* and *Streptococcus* spp. (Khan, 1993).

Amiloride (Figure 1A), an inhibitor of Na<sup>+</sup> transport in Na<sup>+</sup> channels, Na<sup>+</sup>/H<sup>+</sup> exchangers and

Professor Yasuo Imae died of a cerebral haemorrhage on July 2nd, 1993. This article is dedicated to him.

Present address: K. Muramoto, Department of Molecular Biophysics and Biochemistry, Yale University, New Haven, CT 06520-8114, USA.

Abbreviations used: LDM, laser dark-field microscopy; 6-IA, 6-iodoamiloride; r.p.s., revolutions per second.

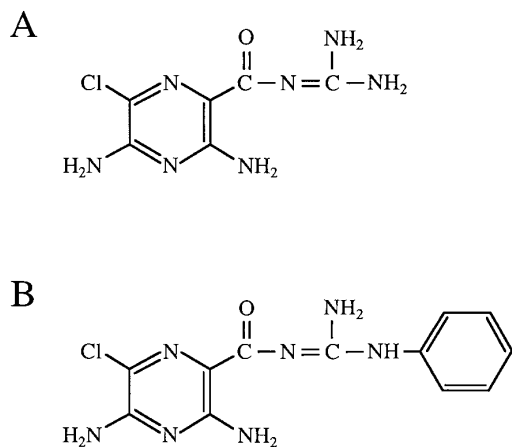


**Figure 1.** The structure of amiloride and phenamil. A, Amiloride. The values of  $IC_{50}$  of amiloride are 0.2  $\mu$ M for Na<sup>+</sup> channel, 84  $\mu$ M for Na<sup>+</sup>/H<sup>+</sup> exchange and 1100  $\mu$ M for Na<sup>+</sup>/Ca<sup>2+</sup> exchange (Cragoe *et al.*, 1992). B, Phenamil. One of the hydrogen atoms of the terminal amino groups of the guanidino moiety in amiloride is substituted by a phenyl group. The potencies of phenamil relative to amiloride are 17 for Na<sup>+</sup> channel,  $\ll 0.1$  for Na<sup>+</sup>/H<sup>+</sup> exchange and 6 for Na<sup>+</sup>/Ca<sup>2+</sup> exchange (Cragoe *et al.*, 1992).

Na<sup>+</sup>/Ca<sup>2+</sup> exchangers (Kleyman & Cragoe, 1988; Cragoe *et al.*, 1992), specifically and reversibly inhibits rotation of the Na<sup>+</sup>-driven motors of alkaliphilic *Bacillus* spp. and *Vibrio* spp. (Sugiyama *et al.*, 1988; Atsumi *et al.*, 1992a,b; Kawagishi *et al.*, 1995). Some amiloride analogs also inhibit the Na<sup>+</sup>-driven motor (Sugiyama *et al.*, 1988). Phenamil (Figure 1B), the most potent inhibitor known at present, completely inhibits the motility of *B. firmus* and *Vibrio alginolyticus* at a concentration of much less than 1 mM. Amiloride and 6-IA were suggested to interact with the Na<sup>+</sup>-binding site at the external surface of the force-generating unit (Sugiyama *et al.*, 1988; Atsumi *et al.*, 1990; Muramoto *et al.*, 1994), and thereby block the Na<sup>+</sup> influx. Analyses of the inhibitory mechanisms of these amiloride analogs should be useful in characterizing the coupling between ion translocation and force generation in the Na<sup>+</sup>-driven motor.

Laser dark-field microscopy (LDM) has been developed to measure flagellar rotation with high temporal resolution (Kudo *et al.*, 1990). In this method, the rotating flagellum is irradiated by a thin laser beam and the rotation rate is measured from the intensity change of the scattered light. Recently, we analyzed the Na<sup>+</sup>-driven polar flagellar rotation of *V. alginolyticus* using LDM and found that the rotation rate was very fast, up to 1700 r.p.s. at 35°C (Magariyama *et al.*, 1994). Rotational fluctuation was also examined, with results that suggested that the fluctuation was mainly caused by rotational Brownian motion (Muramoto *et al.*, 1995). In other words, it appeared that the motor mechanism involved free diffusion.

In the present study, we have used LDM with high temporal resolution to measure flagellar

rotation of *V. alginolyticus* in the presence of amiloride and phenamil. We have found that phenamil causes very large fluctuations in rotation rate, distinct from those caused by rotational Brownian motion. The processes of association and dissociation of inhibitors at sites on the force-generating units were considered to play a major role in the fluctuation.

## Results

### Changes in rotational fluctuation caused by inhibitors

We examined the inhibitory effect of amiloride and phenamil on the Na<sup>+</sup>-driven flagellar motor of *V. alginolyticus* using LDM. Figure 2A, C and E show the intensity change of the scattered light from the rotating flagellum. Figure 2B, D and F show the rotation rates ( $\omega$ ) as a function of time and their histogram. Each value of  $\omega$  was determined as the reciprocal of the peak to peak interval of the intensity change (see equation (2)). Figure 2A and B show the flagellar rotation in the absence of inhibitors (in HG medium (pH 7.0) supplemented with 50 mM NaCl and 250 mM KCl). The flagellum rotated fast and smoothly. The average rotation rate ( $\bar{\omega}$ ) for one second was about 600 r.p.s., and the standard deviation of  $\omega$  ( $\sigma_{\omega}$ ) was about 8% of  $\bar{\omega}$ .

When 1.5 mM of amiloride was added,  $\bar{\omega}$  decreased to about 200 r.p.s. (Figure 2C and D). The value of  $\sigma_{\omega}$  was about 10% of  $\bar{\omega}$ . When 0.6  $\mu$ M phenamil was added,  $\bar{\omega}$  decreased to about 200 r.p.s. (Figure 2E and F), and  $\sigma_{\omega}$  increased substantially. In Figure 2F, for example,  $\omega$  decreased rapidly and markedly from about 200 to 50 r.p.s. at 180 ms and increased from 50 to 200 r.p.s. at 250 ms. The value of  $\sigma_{\omega}$  for one second was about 43% of  $\bar{\omega}$ . This value was much larger than those in the absence of inhibitors or in the presence of amiloride.

Figure 3 shows the changes in  $\omega$  caused by phenamil for five consecutive seconds including the one second period shown in Figure 2F. A large fluctuation in  $\omega$  was seen in every period. The values of  $\bar{\omega}$  for each one second interval in Figure 3A to E were 229, 212, 148, 188 and 232 r.p.s.; and those of  $\sigma_{\omega}$  were 27, 27, 43, 35 and 32% of  $\bar{\omega}$ , respectively. These differences in  $\bar{\omega}$  and  $\sigma_{\omega}$  indicate that one second is rather short for statistical processing of the data. On the contrary, one second is sufficiently long for statistical processing for the inhibition by amiloride, because the values of  $\bar{\omega}$  and  $\sigma_{\omega}$  for any of the one second periods in the measurement were almost the same as those for the period shown in Figure 2D (data not shown). That is, the changes in  $\omega$  induced by phenamil occur more slowly than those induced by amiloride.

### Rotational fluctuation as a function of the inhibitor concentration

Figure 4 shows the effects of amiloride and phenamil on  $\bar{\omega}$  and  $\sigma_{\omega}/\bar{\omega}$  (for five seconds) as

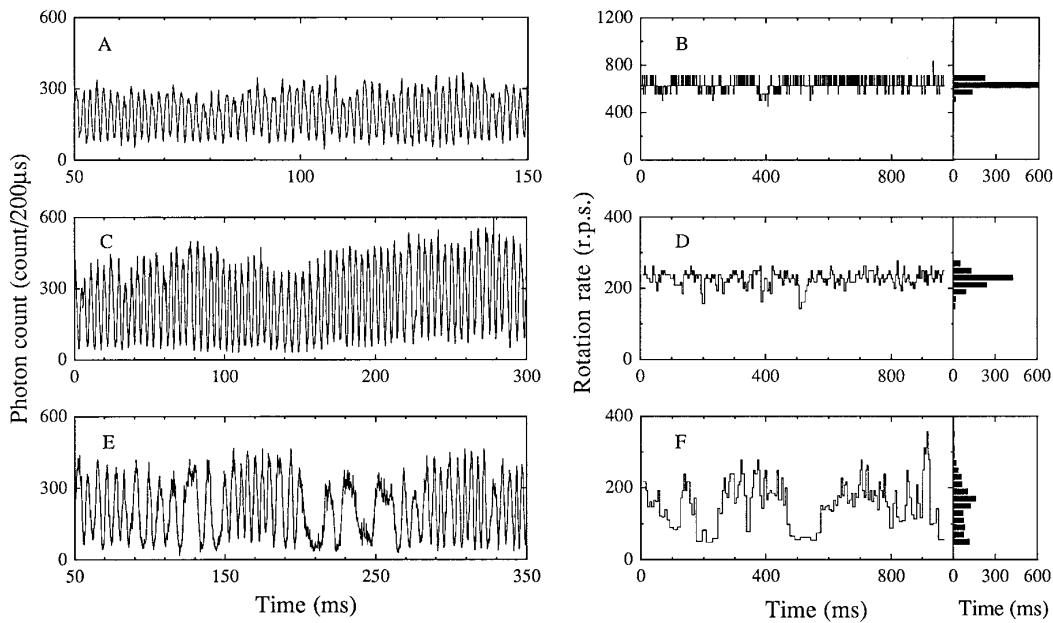


**Figure 2.** Change of rotation rate in the presence of amiloride and phenamil. YM3 cells were prepared in HG medium containing 50 mM NaCl and 250 mM KCl. A and B, In the absence of inhibitor; C and D, in the presence of 1.5 mM amiloride; E and F, in the presence of 0.6  $\mu$ M phenamil. The laser beam was focused on a single freely rotating flagellum on a cell whose body was stuck to a glass surface. A, C and E, The intensity changes of the scattered light from the rotating flagellum. B, D and F, The values of  $\omega$  over a one second interval and their histogram. The resolution was limited by the sampling interval of the light intensity change (200  $\mu$ s), and is seen as the discrete feature of obtained  $\omega$  values.

functions of their concentrations. As shown in Figure 4A,  $\bar{\omega}$  monotonically decreased with increasing concentration of amiloride, with 2 mM amiloride causing more than a 90% decrease in  $\bar{\omega}$ . The value of  $IC_{50}$ , which is the concentration of an inhibitor required for decreasing  $\bar{\omega}$  by 50%, was estimated as about 1 mM for amiloride. The value of  $\sigma_{\omega}/\bar{\omega}$  was about 0.09 in the absence of amiloride, and only slightly increased with increasing concentration of amiloride (Figure 4B). Both  $\bar{\omega}$  and  $\sigma_{\omega}/\bar{\omega}$  varied rather widely from cell to cell, and the distributions seemed to be independent of the presence of the inhibitors.

In the case of phenamil (Figure 4C), the decrease in  $\bar{\omega}$  with increasing concentration of the inhibitor was steeper than that seen with amiloride. Only 2.5  $\mu$ M phenamil was sufficient to cause more than a 90% decline of  $\bar{\omega}$ . The value of  $IC_{50}$  of phenamil was estimated to be about 0.25  $\mu$ M, which was 4000 times smaller than that of amiloride. For swimming speed, similar values of  $IC_{50}$  were obtained for both amiloride and phenamil (data not shown).

Phenamil also caused an increase in  $\sigma_{\omega}/\bar{\omega}$ . The values of  $\sigma_{\omega}/\bar{\omega}$  increased steeply from 0.09 to about 0.4 with increasing concentration of phenamil within the range 0 to 1  $\mu$ M (Figure 4D). Further addition of phenamil caused a gradual increase in  $\sigma_{\omega}/\bar{\omega}$ , reaching up to 0.6 in the presence of 5  $\mu$ M phenamil. Thus, the presence of phenamil caused a decrease in  $\bar{\omega}$  and an increase in the fluctuation in the rotation of flagellar motor, with the magnitude of the fluctuation depending on the concentration of phenamil.

The difference of fluctuation between amiloride and phenamil seems to be caused by a difference between the rates of association and/or dissociation of the inhibitors.

#### Rotational fluctuation after rapid application of the inhibitors

To test whether the fluctuation in  $\omega$  directly reflected the association and dissociation of the inhibitor molecule to the motor, transient effects of the inhibitors on  $\omega$  were examined. A small amount of 3 mM amiloride or 10  $\mu$ M phenamil was rapidly applied to a stuck cell using a microinjector and the changes in  $\omega$  were measured.

Figure 5A shows the change in  $\omega$  upon applying amiloride. In the absence of amiloride, the flagellum rotated at about 420 r.p.s. Within one second after the application of amiloride, the value of  $\omega$  started to decrease, continued to decrease for about 200 ms, and reached a value of about 160 r.p.s. The fluctuation of flagellar rotation during the decreasing process and after reaching the lower level were almost the same as that at the initial level. The duration of the decrease in  $\omega$  probably corresponds to the period required for increasing the concentration of amiloride around the cell after the application. It should be noted that the inhibitor was estimated to arrive at the cell within 0.5 to one second after the injection.

When phenamil was applied (Figure 5B), a sudden decrease in  $\omega$  (to about 250 r.p.s. on average) was observed within one second after the appli-

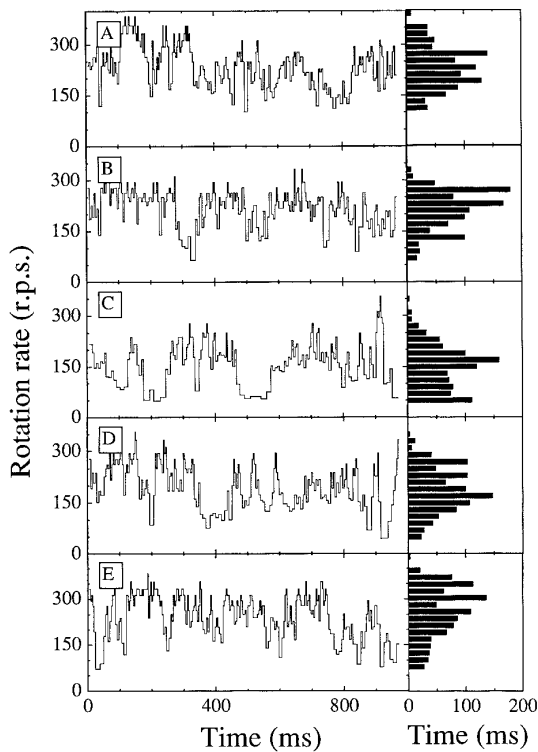


**Figure 3.** Rotation rate over an extended period in the presence of phenamil. Rotation rate changes for five consecutive seconds in the presence of  $0.6 \mu\text{M}$  of phenamil. The values of  $\bar{\omega}$  and  $\sigma_{\omega}$  for each second were: A,  $229 \pm 62$  r.p.s.; B,  $212 \pm 57$  r.p.s.; C,  $148 \pm 63$  r.p.s.; D,  $188 \pm 65$  r.p.s.; and E,  $232 \pm 74$  r.p.s.

cation. At the same time, the rotational fluctuation started to increase. This result suggests that the large fluctuation is due to the direct interaction between phenamil and the motor. Since the concentration of phenamil around the cell presumably increased gradually, as in the case of

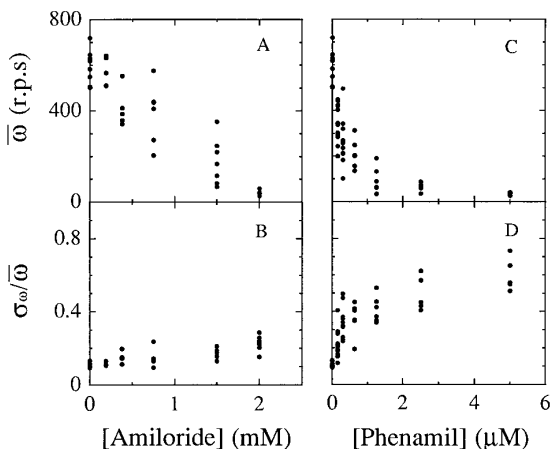


**Figure 4.** Dependence of rotation rate and its fluctuation on amiloride and phenamil concentrations. The values of  $\bar{\omega}$  and  $\sigma_{\omega}/\bar{\omega}$  for five seconds are shown for several cells at each concentration of amiloride (A and B) and phenamil (C and D). Each point indicates the data obtained from an individual cell.

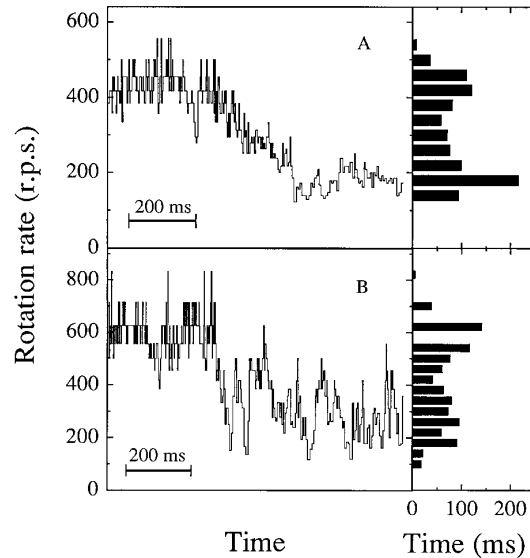


**Figure 5.** Transitional change of rotation rate upon rapid application of (A)  $3 \text{ mM}$  amiloride and (B)  $10 \mu\text{M}$  phenamil in HG medium by a microinjector.

amiloride, the large decrease in  $\bar{\omega}$  and the increase in the fluctuation upon application of phenamil must have occurred at quite low concentrations. This interpretation is consistent with the steep decrease in  $\bar{\omega}$  and increase in  $\sigma_{\omega}/\bar{\omega}$  seen at low concentration of phenamil (Figure 4C and D).

Both with amiloride and with phenamil,  $\bar{\omega}$  and the fluctuation completely recovered to the initial level after the inhibitors were removed (data not shown).

#### Rotational fluctuation at low concentration of inhibitor

If a cell is placed in a very dilute solution of an inhibitor ( $\ll IC_{50}$ ), so that there is only slight inhibition of flagellar rotation, it might be possible to observe events induced by a single inhibitor molecule. As shown in Figure 6A,  $\bar{\omega}$  and its fluctuation in the presence of  $0.2 \text{ mM}$  amiloride (corresponding to 20% of  $IC_{50}$ ) were almost equal to those in the absence of amiloride (Figure 2B).

Figure 6B to D shows the changes in  $\bar{\omega}$  in the presence of  $0.04 \mu\text{M}$  phenamil (corresponding to 16% of  $IC_{50}$ ). The values of  $\bar{\omega}$  and its fluctuation were generally similar to those observed in the absence of inhibitors. However, rapid and large decreases in  $\bar{\omega}$  with short duration (50 to 300 ms) were occasionally observed (Figure 6B, at 350 ms; C, at 700 ms; D, at 50, 500, and 800 ms). The durations of periods of decreasing  $\bar{\omega}$  were different from one another and were considered to directly reflect the binding durations of phenamil to the motor. Their values suggest that dissociation of the inhibitor from the motor is slow.

Since the concentration of phenamil was very low and there were rather long periods in which  $\bar{\omega}$  was not affected, the decreases in  $\bar{\omega}$  in Figure 6B to D

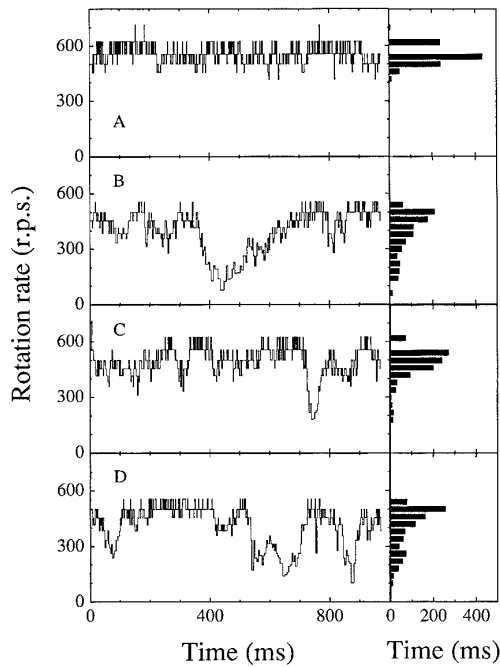


**Figure 6.** Changes of rotation rate in the presence of low concentration of amiloride and phenamil. Stuck YM3 cells were prepared in HG medium containing 50 mM NaCl, 250 mM KCl and 0.2 mM amiloride (A) or 0.04  $\mu$ M phenamil (B to D).

were considered to be induced by a single phenamil molecule. However, the decreases in  $\omega$  were unexpectedly large, frequently more than 70% (for example,  $\omega$  suddenly dropped from 450 r.p.s. to 150 r.p.s. at 350 ms in Figure 6B).

### Cell growth in the presence of the inhibitor

To preclude the possibility that the changes in rotation rate and its fluctuation are secondary effects of cell damage, we examined cell growth in the presence of phenamil. Although the motility of YM3 cells was completely inhibited by 100  $\mu$ M phenamil, cell growth was unaffected (data not shown). It has been reported that 2 mM amiloride, which almost completely inhibits the motility of *V. alginolyticus*, does not affect membrane potential and inhibits cell growth only slightly (Atsumi *et al.*, 1992a). We conclude that, at the concentrations used, phenamil did not affect cellular physiology and amiloride did not severely affect it, and that the changes in  $\omega$  and its fluctuation were not secondary effects but the results of direct interaction of the inhibitors with the motor. The facts that the decreases in  $\omega$  were observed immediately after inhibitor addition (Figure 5) and that phenamil affected  $\omega$  even at very low concentrations (Figure 6) were consistent with the idea.

### Computer simulation of the inhibition process

To analyze the relation between the inhibition of the motor rotation and its fluctuation, we carried out

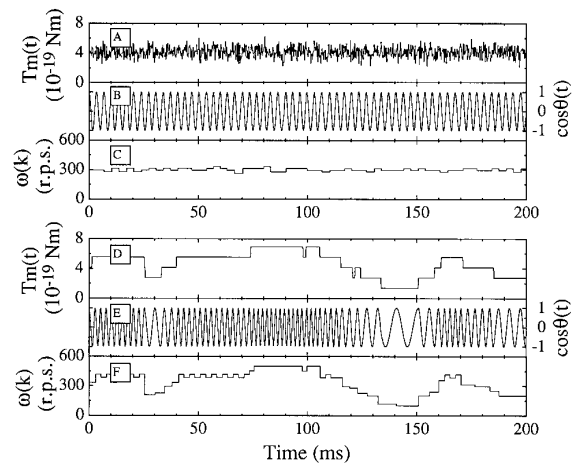


**Figure 7.** Examples of the results of the simulation. The simulations were carried out based on equations (5a) and (6) to (9) using the following parameters:  $N_0 = 6$  (Muramoto *et al.*, 1994),  $f = 2.2 \times 10^{-22}$  Nms (Muramoto *et al.*, 1995),  $T_0 = 1.4 \times 10^{-19}$  Nm (Magariyama *et al.*, 1995); A to C,  $IC_{50} = 1.0 \times 10^{-3}$  M,  $k_+ = 10^8$  M<sup>-1</sup> s<sup>-1</sup>,  $k_- = 10^5$  s<sup>-1</sup> and  $I = 1.6$  mM (corresponding to the inhibition by amiloride); D to F,  $IC_{50} = 2.5 \times 10^{-7}$  M,  $k_+ = 10^8$  M<sup>-1</sup> s<sup>-1</sup>,  $k_- = 25$  s<sup>-1</sup> and  $I = 0.5$   $\mu$ M (corresponding to the inhibition by phenamil). Data were calculated for time intervals  $\Delta t$  of 1  $\mu$ s. The values of  $T_m(t)$  and  $\cos \theta(t)$  averaged over 200 such intervals are shown. The values of  $\bar{\omega}(k)$  and  $\sigma_{\omega(k)}$  for one second were: A to C,  $300 \pm 14$  r.p.s.; D to F,  $258 \pm 113$  r.p.s.

computer simulation of the kinetics of inhibition of the motor (for details, see Materials and Methods). We made the following assumptions: (1) The motor has multiple force-generating units, each of which functions independently, and the torque generated by a motor is the sum of the torque generated by each unit (Block & Berg, 1984; Blair & Berg, 1988; Muramoto *et al.*, 1994). (2) An inhibitor binds to a force-generating unit with intrinsic rate constants of association ( $k_+$ ) and dissociation ( $k_-$ ; Sugiyama *et al.*, 1988; Atsumi *et al.*, 1990, 1992b). (3) The force-generating unit bound by an inhibitor molecule generates no torque (Sugiyama *et al.*, 1988; Atsumi *et al.*, 1990, 1992b).

The simulation was carried out for several pairs of  $k_+$  and  $k_-$  values, which are related to each other through  $IC_{50}$  within the framework of the present model as follows:

$$k_- = k_+ IC_{50} \quad (1)$$

For the inhibition by amiloride and phenamil,  $IC_{50}$  of 1 mM and 0.25  $\mu$ M were used, respectively.

Figure 7A to C shows an example of the calculated results of inhibition by amiloride ( $IC_{50} = 1$  mM,  $k_+ = 10^8$  M<sup>-1</sup> s<sup>-1</sup>,  $k_- = 10^5$  s<sup>-1</sup>, and  $I = 1.6$  mM). Both binding and release of amiloride occurred within much shorter times than the rotation period, which resulted in frequent changes of instantaneous torque,  $T_m(t)$  (Figure 7A). Consequently, the changes in  $T_m(t)$  were averaged in each revolution. That is, changes in  $\bar{\omega}(k)$  determined from the peak intervals of  $\cos \theta$  in Figure 7B were rather small (Figure 7C).

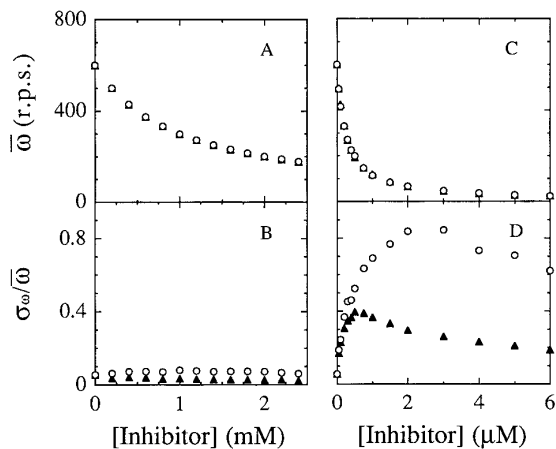


**Figure 8.** Simulated rotation rate and its fluctuation as functions of inhibitor concentrations. Results of the simulation are summarized. Parameters used were: A and B,  $IC_{50} = 1.0 \times 10^{-3}$  M; open circle,  $k_+ = 10^7$  M<sup>-1</sup> s<sup>-1</sup>,  $k_- = 10^4$  s<sup>-1</sup>, filled triangle,  $k_+ = 10^8$  M<sup>-1</sup> s<sup>-1</sup>,  $k_- = 10^5$  s<sup>-1</sup>. C and D,  $IC_{50} = 2.5 \times 10^{-7}$  M; open circle,  $k_+ = 10^8$  M<sup>-1</sup> s<sup>-1</sup>,  $k_- = 25$  s<sup>-1</sup>, filled triangle,  $k_+ = 10^9$  M<sup>-1</sup> s<sup>-1</sup>,  $k_- = 250$  s<sup>-1</sup>. Values of  $\bar{\omega}$  and  $\sigma_{\omega}/\bar{\omega}$  were calculated for one second (A and B) and for five seconds (C and D).

Figure 7D to F shows calculated results for phenamil ( $IC_{50} = 0.25$   $\mu$ M,  $k_+ = 10^8$  M<sup>-1</sup> s<sup>-1</sup>,  $k_- = 25$  s<sup>-1</sup>, and  $I = 0.5$   $\mu$ M). In this case, the frequency of binding and release of the inhibitor was much lower than that for amiloride (Figure 7D), and the change of  $T_m(t)$  appeared as a large fluctuation in  $\omega(k)$  (Figure 7F). The basic features of calculated changes of  $\omega(k)$  for amiloride and phenamil were consistent with those of the experimental results shown in Figure 2D and F.

As summarized in Figure 8, the results of simulation showed features of  $\bar{\omega}$  and  $\sigma_{\omega}/\bar{\omega}$  essentially similar to those obtained experimentally (Figure 4: for details, see Discussion). Since calculated values of  $\bar{\omega}$  were independent of the values of  $k_+$  and  $k_-$ , appropriate values of  $k_+$  and  $k_-$  were evaluated by comparing calculated values of  $\sigma_{\omega}/\bar{\omega}$  with the experimental ones. In the case of amiloride, appropriate values of  $k_+$  and  $k_-$  were estimated to be  $10^7$  to  $10^8$  M<sup>-1</sup> s<sup>-1</sup> and  $10^4$  to  $10^5$  s<sup>-1</sup>, respectively. In the case of phenamil, they were  $10^8$  to  $10^9$  M<sup>-1</sup> s<sup>-1</sup> and 25 to 250 s<sup>-1</sup>, respectively.

## Discussion

Here, we used LDM to examine the inhibition of the Na<sup>+</sup>-driven motor in *V. alginolyticus* by amiloride and phenamil. The values of  $IC_{50}$  of amiloride and phenamil were determined to be 1 mM and 0.25  $\mu$ M, respectively (Figure 4A and C), and so the potency of phenamil is 4000 times larger than that of amiloride. The fluctuation in rotation rate induced by phenamil was much larger than that induced by amiloride (Figure 4B and D). Much slower dissociation of phenamil than amiloride was suggested to cause the differences.

The effects of inhibitors on the motor rotation

were analyzed by a simple kinetic model. Results of computer simulation using this model could explain the essential features of the experimental results. Values of association and dissociation constants of inhibitors to the motor were estimated as:  $k_+ = 10^7$  to  $10^8$  M<sup>-1</sup> s<sup>-1</sup> and  $k_- = 10^4$  to  $10^5$  s<sup>-1</sup> for amiloride; and  $k_+ = 10^8$  to  $10^9$  M<sup>-1</sup> s<sup>-1</sup> and  $k_- = 25$  to 250 s<sup>-1</sup> for phenamil, respectively. The smaller  $IC_{50}$  value for phenamil was reflected as a smaller  $k_-$  value, i.e. slower dissociation, compared with that for amiloride. With millisecond temporal resolution of LDM, the dissociation of phenamil was slow enough that it could be observed, whereas that of amiloride could not.

The simulation did not include the effects of other fluctuations observed in the absence of inhibitors, which are thought to be caused mainly by rotational Brownian motion of the flagellar filament (Muramoto *et al.*, 1995). In the case of amiloride, the experimental values of  $\sigma_{\omega}/\bar{\omega}$  were two to four times larger than the calculated one and slightly increased with increasing inhibitor concentration, while the calculated values remained almost constant (Figures 4B and 8B). If the contribution of the Brownian motion together with the instrumental uncertainty (Muramoto *et al.*, 1995) are added to the calculated  $\sigma_{\omega}/\bar{\omega}$ , the magnitude and slight increase of  $\sigma_{\omega}/\bar{\omega}$  obtained experimentally can be well explained. In the case of phenamil, the magnitude of fluctuation induced by the inhibitor is sufficiently large that the contribution of other fluctuations can be neglected in the present analysis.

Although the basic features of the experimental results could be explained by the present model, the detailed dependence of  $\sigma_{\omega}/\bar{\omega}$  on the concentration of phenamil is different between Figures 4D and 8D. Furthermore, in the presence of low concentrations of phenamil, the rotation rate slowed remarkably (Figure 6). The binding of a single phenamil molecule might decrease  $\omega$  much more than is predicted by the model, or it might be necessary to consider co-operative interaction between phenamil and the motor. In the former case, binding of phenamil to a force-generating unit may cause a block of the Na<sup>+</sup> influx through the unit and other effects, such as inactivation of other units or additional drag torque in the motor. If inactivation of other units occurs, the large slowdown at low concentrations of phenamil would be observed also under high-load conditions. On the contrary, if phenamil induces only the additional drag torque in the motor, the large slowdown would not be observed under such conditions, because  $\omega$  is mainly determined by the larger external drag torque. Hence analysis of the slowdown under high-load conditions, e.g., observation of tethered-cell rotation with high temporal resolution, is desired to further understand the inhibitory mechanism of phenamil.

In a previous study, we used the photoreactive amiloride analog, 6-IA, to successively inactivate the force-generating units of the Na<sup>+</sup>-driven motor in

*B. firmus* (Muramoto *et al.*, 1994). Without UV irradiation, the inhibitory effect of 6-IA was similar to that of amiloride. Photoactivation of 6-IA caused an irreversible and stepwise decrease of the rotation rate of tethered cells. In this case, the sizes of speed drops were roughly equal in each step and the number of steps was estimated to be from five to nine. These results suggest that irreversible binding of 6-IA merely causes a block of the Na<sup>+</sup> influx through the unit or the increase in drag caused by binding of 6-IA, if any, is much smaller than the drag on the rotating cell body.

The features of rotational fluctuation induced by amiloride and phenamil were remarkably different. The estimated dissociation constants had different orders of magnitude. Phenamil is more hydrophobic than amiloride, and hence might strongly interact with the hydrophobic region in the force-generating unit, or more easily permeate through the cytoplasmic membrane and interact with internal Na<sup>+</sup>-binding sites of the force-generating units, which were suggested by Yoshida *et al.* (1990). Previous studies reported that the inhibition by amiloride is competitive with external Na<sup>+</sup>, while inhibition by phenamil is non-competitive (Sugiyama *et al.*, 1988; Atsumi *et al.*, 1990). The interaction between amiloride analogs and proteins, such as various Na<sup>+</sup>-transporters and anti-amiloride antibody, has been studied (Cragoe *et al.*, 1992; Lin *et al.*, 1994). Negulyaev and Vedernikova (1994) showed, by using single patch measurements, that the blocking mechanisms of amiloride and its derivative ethylisopropylamiloride are different. The Na<sup>+</sup> channels in epithelial cells have been proposed to have one or more drug-binding sites (Lane *et al.*, 1991).

Recently, in *V. parahaemolyticus*, two genes encoding components of the polar flagellar motor, which might be the force-generating unit, have been identified (McCarter 1994a, 1994b). In *V. alginolyticus*, a procedure for electroporation was established (Kawagishi *et al.*, 1994), and genes for motility have been cloned (Okunishi *et al.*, 1996). Because amiloride and phenamil inhibited the motor rotation in distinct manners, it might be possible to isolate the mutants whose sensitivities to amiloride and phenamil are different. The analyses of such mutants would provide important clues to the identification and characterization of the proteins that play important roles in the force-generating units, and hence the force-generation mechanism of the flagellar motor.

## Materials and Methods

### Bacterial strain and media

A smooth-swimming mutant of *V. alginolyticus*, YM3, was used (Muramoto *et al.*, 1995). Heart Infusion (HI) broth contained 25 g of heart infusion broth (Difco) and 15 g of NaCl per liter of distilled water. HG medium contained 50 mM Hepes-KOH (pH 7.0), 5 mM glucose and 5 mM MgCl<sub>2</sub>. Amiloride (Sigma Chemical Co.,

St Louis, MO) and phenamil (provided by T. Atsumi of Suzuka College of Technology) were dissolved in dimethylsulfoxide and stored at -20°C.

### Preparation of stuck cells and measurement of rotation rate of a single flagellum

YM3 cells were grown at 30°C with shaking in HI broth and harvested during the late logarithmic phase of growth. Cells from 1 ml of culture were washed by centrifugation in HG medium supplemented with 50 mM NaCl and 250 mM KCl, and resuspended in 5 ml of the same medium.

“Stuck cells” whose bodies were fixed to a glass surface and whose flagella rotated freely were prepared as described (Muramoto *et al.*, 1995). Rotation rate of a single flagellum on a cell attached to the coverslip was measured by LDM according to Kudo *et al.* (1990) and Muramoto *et al.* (1995). The rotation period ( $\tau(k)$ ) for the  $k$ th revolution was determined from the peak to peak interval of the LDM data, and the rotation rate ( $\omega(k)$ ) for the  $k$ th revolution was calculated as:

$$\omega(k) = \frac{1}{\tau(k)} \quad (2)$$

All measurements were made at room temperature.

### Analysis of rotational fluctuation

The statistical values used in this study were calculated as follows:

$$\bar{\omega} = \frac{\sum_{k=1}^N \omega(k)\tau(k)}{\sum_{k=1}^N \tau(k)} = \frac{N}{t_0} \quad (3)$$

$$\sigma_{\omega} = \sqrt{\frac{\sum_{k=1}^N \{\omega(k) - \bar{\omega}\}^2 \tau(k)}{\sum_{k=1}^N \tau(k)}} = \sqrt{\frac{\sum_{k=1}^N \omega(k)}{t_0} - \bar{\omega}^2} \quad (4)$$

Here,  $t_0$  is the duration of the measurement,  $\bar{\omega}$  is the average of the rotation rate ( $\omega$ ) for the duration,  $N$  is the total number of revolutions, and  $\sigma_{\omega}$  is the standard deviation of  $\omega$ .

### Rapid application of inhibitor around a cell

Stuck YM3 cells were prepared in HG medium containing 50 mM NaCl and 250 mM KCl. A thin glass capillary was filled with the same medium supplemented with 3 mM amiloride or 10  $\mu$ M phenamil. The capillary was inserted into the space between the glass slide and the cover slip, where the stuck cell was prepared. The capillary was placed with its tip near the stuck cell, on the side opposite from the flagellum, and was oriented parallel with the flagellum. The inhibitor was flushed toward the stuck cell with a microinjector (CIJ-1; Shimadzu, Tokyo, Japan). The HG medium around the cell was flowed slowly parallel with the direction of injection during the measurement.

### Computer simulation of the inhibition of the motor

We assumed that the motor has independently functioning force-generating units, each of which is inactivated by binding of inhibitors. The torque generated by the motor at time  $t$ ,  $T_m(t)$ , is given by summing the torque generated by each unit as follows:

$$T_m(t) = \{N_u - n_u(t)\} T_0 \quad (5a)$$

Here,  $N_u$  is total number of the force-generating units in a motor,  $n_u(t)$  is the number of the inactivated force-generating units at time  $t$ , and  $T_0$  is the torque generated by a functioning unit. In equation (5a), torque generated by the motor was assumed to be independent of the rotation rate (Washizu *et al.*, 1993; Berg & Turner, 1993). It should be noted that other experiments indicated the torque to linearly decrease with the rotation rate (Lowe *et al.*, 1987; Iwazawa *et al.*, 1993). The motor torque is expressed as:

$$T_m(t) = \{N_u - n_u(t)\} T_0 - \frac{T_0}{\omega_0} \omega \quad (5b)$$

Here  $T_0$  is the zero-rotation-rate torque generated by a functioning unit and  $\omega_0$  is the zero-torque rotation rate. However, the results of simulation using equation (5b) is essentially equivalent to those using equation (5a). Hence we adopted simpler torque characteristic (equation (5a)) in the present study.

To determine the value of  $n_u(t)$  of equation (5a) in the simulation, we considered the transition probabilities for a force-generating unit from active to inactive state ( $P_+$ ) and inactive to active state ( $P_-$ ) in  $\Delta t$ :

$$P_+ = k_+ I \Delta t \quad (6)$$

$$P_- = k_- \Delta t \quad (7)$$

Here,  $I$  is a concentration of an inhibitor in the medium, and  $k_+$  and  $k_-$  are rate constants of association and dissociation of inhibitors to the force-generating units, respectively. In the simulation, a random number from 0 to 1 was generated by a computer for each force-generating unit. If a force-generating unit was active and the random number was smaller than  $P_+$ , the state of the unit was changed from active to inactive. On the contrary, if a unit was inactive and the number was smaller than  $P_-$ , the state was changed from inactive to active. The value of  $n_u(t)$  was determined as the resultant number of inactive units. The value was determined on every time-step  $\Delta t$ , where the value of  $\Delta t$  was set as  $10^{-6}$  second.

The rotation angle of the motor at time  $t$ ,  $\theta(t)$ , and the average rotation rate for the  $k$ th revolution,  $\omega(k)$ , are given by the following equations:

$$\theta(t + \Delta t) = \theta(t) + \frac{T_m(t)}{f} \Delta t \quad (8)$$

$$\omega(k) = \frac{1}{t_{\theta=2k\pi} - t_{\theta=2(k-1)\pi}} \quad (9)$$

Here,  $f$  is the rotational frictional drag coefficient of the flagellar filament (Holwill & Burge, 1963; Magariyama *et al.*, 1995), and  $t_{\theta=2k\pi}$  is time when  $\theta(t)$  is  $2k\pi$  (see Figure 7).

### Acknowledgements

We thank F. Oosawa and H. Hotani for support and discussion, T. Atsumi for providing reagent, and R. M. Macnab for critical reading of the manuscript. This work

was partly supported by grants-in-aid for scientific researches (to K.M., I.K., and M.H.) from the Ministry of Education, Science and Culture of Japan.

### References

- Atsumi, T., Sugiyama, S., Cragoe, E. J., Jr & Imae, Y. (1990). Specific inhibition of the Na<sup>+</sup>-driven flagellar motors of alkalophilic *Bacillus* strains by the amiloride analog phenamil. *J. Bacteriol.* **172**, 1634–1639.
- Atsumi, T., Maekawa, Y., Tokuda, H. & Imae, Y. (1992a). Amiloride at pH 7.0 inhibits the Na<sup>+</sup>-driven flagellar motors of *Vibrio alginolyticus* but allows the cell growth. *FEBS Letters*, **314**, 114–116.
- Atsumi, T., McCarter, L. & Imae, Y. (1992b). Polar and lateral flagellar motors of marine *Vibrio* are driven by different ion-motive forces. *Nature*, **355**, 182–184.
- Berg, H. C. & Turner, L. (1993). Torque generated by the flagellar motor of *Escherichia coli*. *Biophys. J.* **65**, 2201–2216.
- Blair, D. F. & Berg, H. C. (1988). Restoration of torque in defective flagellar motors. *Science*, **242**, 1678–1681.
- Blair, D. F. (1990). The bacterial flagellar motor. *Semi. Cell Biol.* **1**, 75–85.
- Block, S. M. & Berg, H. C. (1984). Successive incorporation of force-generating units in the bacterial rotary motor. *Nature*, **309**, 470–472.
- Chernyak, B. V., Dibrov, P. A., Glagolev, A. N., Sherman, M. Yu. & Skulachev, V. P. (1983). A novel type of energetics in a marine alkali-tolerant bacterium.  $\Delta\bar{u}$ Na<sup>+</sup>-driven motility and sodium cycle. *FEBS Letters*, **164**, 38–42.
- Cragoe, E. J., Jr, Kleyman, T. R. & Simchowitz, L. (1992). *Amiloride and its Analogs. Unique Cation Transport Inhibitors*, VCH Publishers, Inc., New York.
- Hirota, N., Kitada, M. & Imae, Y. (1981). Flagellar motors of alkalophilic *Bacillus* are powered by an electrochemical potential gradient of Na<sup>+</sup>. *FEBS Letters*, **132**, 278–280.
- Holwill, M. E. J. & Burge, R. E. (1963). A hydrodynamic study of the motility of flagellated bacteria. *Arch. Biochem. Biophys.* **101**, 249–260.
- Imae, Y. & Atsumi, T. (1989). Na<sup>+</sup>-driven bacterial flagellar motors. *J. Bioenerg. Biomembr.* **21**, 705–716.
- Iwazawa, J., Imae, Y. & Kobayashi, S. (1993). Study of the torque of the bacterial flagellar motor using a rotating electric field. *Biophys. J.* **64**, 925–933.
- Jones, C. J. & Aizawa, S.-I. (1991). The bacterial flagellum and flagellar motor: structure, assembly and function. *Advan. Microb. Phys.* **32**, 110–172.
- Kawagishi, I., Okunishi, I., Homma, M. & Imae, Y. (1994). Removal of the periplasmic DNase before electroporation enhances efficiency of transformation in the marine bacterium *Vibrio alginolyticus*. *Microbiology*, **140**, 2355–2361.
- Kawagishi, I., Maekawa, Y., Atsumi, T., Homma, M. & Imae, Y. (1995). Isolation of the polar and lateral flagellum-defective mutants in *Vibrio alginolyticus* and identification of their flagellar driving energy sources. *J. Bacteriol.* **177**, 5158–5160.
- Khan, S. (1993). Gene to ultrastructure: the case of the flagellar basal body. *J. Bacteriol.* **175**, 2169–2174.
- Kleyman, T. R. & Cragoe, E. J., Jr (1988). Amiloride and its analogs as tool in the study of ion transport. *J. Membr. Biol.* **105**, 1–21.
- Kudo, S., Magariyama, Y. & Aizawa, S.-I. (1990). Abrupt changes in flagellar rotation observed by laser dark-field microscopy. *Nature*, **346**, 677–680.

- Lane, J. W., McBride, D. W. & Hamill, O. P. (1991). Amiloride block of mechanosensitive cation channel in *Xenopus oocytes*. *J. Physiol.* **441**, 347–366.
- Lin, C., Kieber-Emmons, T., Villalobos, A. P., Foster, M. H., Wahlgren, C. & Kleyman T. R. (1994). Topology of an amiloride-binding protein. *J. Biol. Chem.* **269**, 2805–2813.
- Lowe, G., Meister, M. & Berg, H. C. (1987). Rapid rotation of flagellar bundles in swimming bacteria. *Nature*, **325**, 637–640.
- Magariyama, Y., Sugiyama, S., Muramoto, K., Maekawa, Y., Kawagishi, I., Imae, Y. & Kudo, S. (1994). Very fast flagellar rotation. *Nature*, **371**, 752.
- Magariyama, Y., Sugiyama, S., Muramoto, K., Kawagishi, I., Imae, Y. & Kudo, S. (1995). Simultaneous measurement of bacterial flagellar rotation rate and swimming speed. *Biophys. J.* **61**, 2154–2162.
- Manson, M. D., Tedesco, P., Berg, H. C., Harold, F. M. & van der Drift, C. (1977). A protonmotive force drives bacterial flagella. *Proc. Natl Acad. Sci. USA*, **74**, 3060–3064.
- Matsuura, S., Shioi, J.-I. & Imae, Y. (1977). Motility in *Bacillus subtilis* driven by an artificial protonmotive force. *FEBS Letters*, **82**, 187–190.
- McCarter, L. L. (1994a). MotY, a component of the sodium-type flagellar motor. *J. Bacteriol.* **176**, 4219–4225.
- McCarter, L. L. (1994b). MotX, the channel component of the sodium-type flagellar motor. *J. Bacteriol.* **176**, 5988–5998.
- Muramoto, K., Sugiyama, S., Cragoe, E. J., Jr & Imae, Y. (1994). Successive inactivation of the force-generating units of sodium-driven bacterial flagellar motors by a photoreactive amiloride analog. *J. Biol. Chem.* **269**, 3374–3380.
- Muramoto, K., Kawagishi, I., Kudo, S., Magariyama, Y., Imae, Y. & Homma, M. (1995). High-speed rotation and speed stability of sodium-driven flagellar motor in *Vibrio alginolyticus*. *J. Mol. Biol.* **251**, 50–58.
- Negulyaev, Y. A. & Vedernikova, E. A. (1994). Sodium-selective channels in membranes of rat macrophages. *J. Membr. Biol.* **138**, 37–45.
- Okunishi, I., Kawagishi, I. & Homma, M. (1996). Cloning and characterization of *motY*, a gene coding for a component of the sodium-driven flagellar motor in *Vibrio alginolyticus*. *J. Bacteriol.* **178**, 2409–2415.
- Sugiyama, S., Cragoe, E. J., Jr & Imae, Y. (1988). Amiloride, a specific inhibitor for the Na<sup>+</sup>-driven flagellar motors of alkalophilic *Bacillus*. *J. Biol. Chem.* **263**, 8215–8219.
- Yoshida, S., Sugiyama, S., Hojo, Y., Tokuda, H. & Imae, Y. (1990). Intracellular Na<sup>+</sup> kinetically interferes with the rotation of Na<sup>+</sup>-driven flagellar motors of *Vibrio alginolyticus*. *J. Biol. Chem.* **265**, 20346–20350.
- Washizu, M., Kurahashi, Y., Iochi, H., Kurosawa, O., Aizawa, S.-I., Kudo, S., Magariyama, Y. & Hotani, H. (1993). Dielectrophoretic measurement of bacterial motor characteristics. *IEEE Trans. Indust. Appl.* **29**, 286–294.

**Edited by J. Karn**

(Received 12 January 1996; received in revised form 28 March 1996; accepted 2 April 1996)